

Analysis of magnetization and a spin state crossover in the multiferroic $\text{Ca}_3\text{Co}_{2-x}\text{Mn}_x\text{O}_6$

R. Flint,* H.-T. Yi, P. Chandra, S.-W. Cheong, and V. Kiryukhin
*Department of Physics and Astronomy and Center for Emergent Materials,
Rutgers University, Piscataway, NJ 08855, U.S.A.*
(Dated: May 10, 2010)

$\text{Ca}_3\text{Co}_{2-x}\text{Mn}_x\text{O}_6$ ($x \sim 0.96$) is a multiferroic with spin-chains of alternating Co^{2+} and Mn^{4+} ions. The spin state of Co^{2+} remains unresolved, due to a discrepancy between high temperature X-ray absorption ($S = \frac{3}{2}$) and low temperature neutron ($S = \frac{1}{2}$) measurements. Using a combination of magnetic modeling and crystal-field analysis, we show that the existing low temperature data cannot be reconciled within a high spin scenario by invoking spin-orbit or Jahn-Teller distortions. To unify the experimental results, we propose a spin-state crossover with specific experimental predictions.

PACS numbers: 77.80.-e, 75.10.Pq, 75.80.+q, 71.70.-d, 75.30.Wx

Multiferroics where the spin-lattice coupling arises from symmetric superexchange offer great promise for large magnetoelectric effects¹. $\text{Ca}_3\text{Co}_{2-x}\text{Mn}_x\text{O}_6$ ($x \sim 0.96$) (CCMO) is one such material^{1–10}, consisting of anisotropic spin chains where the $\uparrow\uparrow\downarrow\downarrow$ ordering of alternating Co^{2+} and Mn^{4+} spins breaks inversion symmetry. Understanding the magnetic properties is key to understanding the multiferroicity; however, the spin state of the Co^{2+} ions remains unresolved. Here we address this problem directly. High temperature (T) susceptibility (χ)² and X-ray absorption ($T \sim 300\text{K}$) spectroscopy (XAS) measurements⁶, along with first principles calculations,^{6,7} indicate it is in a high spin (HS) ($S = \frac{3}{2}$) state with a large orbital moment ($1.7\mu_B$), whereas low T neutron studies⁴ are consistent with $S = \frac{1}{2}$. In this paper, we demonstrate that the measured high-field magnetization⁵ ($m(H)$) confirms the small moment at low T , and new χ measurements indicate that the moment anisotropy increases with decreasing temperature. One might think that the Co ion remains in the HS state, but that its effective spin is reduced at low T . Here we use a combination of magnetic modeling and crystal-field (CF) analysis to show that no perturbation of the $S = 3/2$ states can account for both the observed moment and the large anisotropy at low T , thereby ruling out this simple picture. In order to resolve the experimental situation, we propose a spin-state crossover for the Co^{2+} ion. Low T XAS measurements would test our proposal directly, and we also predict a number of other experimental consequences.

CCMO consists of c-axis chains of Co^{2+} and Mn^{4+} ions, arranged in a triangular lattice⁴. These atoms reside in alternating octahedral and trigonal prismatic oxygen cages; Mn preferentially sits on the octahedral sites. Magnetic $\uparrow\uparrow\downarrow\downarrow$ order develops along the chains at $T^* = 16\text{K}$. Exchange striction causes alternating bonds to constrict and lengthen. As the two ions have different charges, a macroscopic c-axis polarization results⁴. Comparison of the χ parallel and perpendicular to the chains indicates that these spins have an Ising anisotropy that increases with decreasing T (see Fig. 1).

We now turn to the spin states of the magnetic ions.

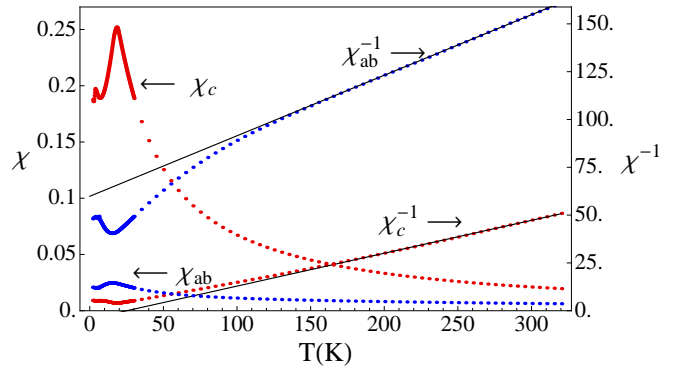


FIG. 1: Susceptibility along the a- and c-axes, indicating increasing Ising anisotropy with decreasing temperature. Sample preparation described in Choi et al⁴.

Mn^{4+} is a $3d^3$ ion in an octahedral environment. The t_{2g} orbital is half-filled, quenching the angular momentum; thus Mn^{4+} acts as a $S = \frac{3}{2}$ Heisenberg spin, consistent with both low- T neutrons⁴ and high- T XAS⁶. This spin state is stable against both spin-orbit (SO) coupling and structural distortions up to the CF splitting $\sim 1\text{ eV}$.

Thus both the anisotropy and the small moment of CCMO at low T must be due to the Co. Co^{2+} is a $3d^7$ ion with three holes in a trigonal prismatic environment. The CF levels, shown in Fig. 2A, are labeled by their L_z quantum numbers¹⁴. While Hund's rules and the CFs are compatible in Mn^{4+} , here they compete. Hund's rules align the holes to yield $S = \frac{3}{2}$, while the CF energy is reduced by placing all three holes in the lowest level to get $S = \frac{1}{2}$. Both scenarios have partially filled levels resulting in orbital moments and anisotropy. We must thus rely on experiment to discern the spin state of Co^{2+} . Curie-Weiss fits to χ , for $T \gg T^*$ yield an effective moment of $\mu_{eff} \sim 6.0\mu_B$ indicating that both Mn^{4+} and Co^{2+} are in the high-spin (HS) $S = \frac{3}{2}$ states^{2,3}, consistent with room T XAS studies⁶. However the moment measured by neutron scattering for $T < T^*$, $0.66\mu_B/\text{Co}$, is significantly less than that expected for the HS sce-

nario, suggesting a LS state⁴. There is a clear discrepancy between these results, and we turn to another low T measurement, $m(H)$, to resolve this issue.

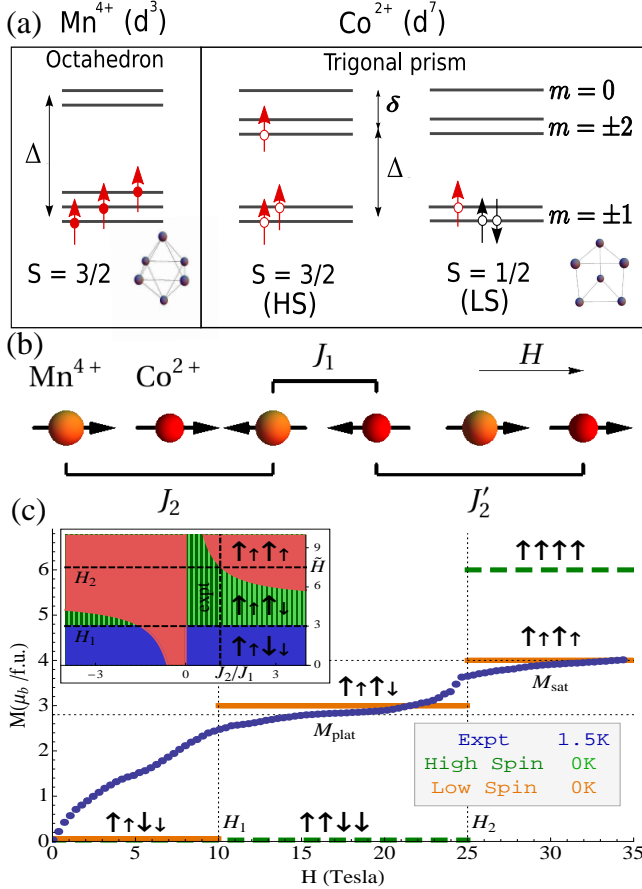


FIG. 2: (a) Crystal field levels and occupations for (Left) Mn⁴⁺ in an octahedral environment where the t_{2g} level is half-filled; the orbital angular momentum is thus quenched and Mn⁴⁺ has a $S = \frac{3}{2}$ Heisenberg spin. (Right) Co²⁺ is simply described by three holes, with the crystal fields inverted from the electron picture. In the trigonal environment, there is a competition between the crystal field splitting and the Hund's rule coupling. Both high- and low-spin ground states have unquenched angular momentum ($\langle L_z \rangle = 2$ and 1 respectively) and are possible. (b) Magnetic structure of the Co²⁺-Mn⁴⁺ chains, showing the in-chain couplings. (c) High field magnetization data (at 1.5K) reproduced from⁵, overlaid with the LS and HS Co cases at $T = 0$. (Inset) Example $T = 0$ phase diagram of the alternating spin ANNNI model ($s = \frac{1}{2}, S = \frac{3}{2}, J'_2/J_2 = 5$), where $\tilde{H} = \frac{H}{g\mu_B J_2}$ and J_2/J_1 are varied. For $3 < J'_2/J_2 < 6$, the experimental ratio $H_2/H_1 \sim 2.5$ requires $J_1 > 0$, while for $J'_2/J_2 > 6$, $J_1 < 0$. Any first principles calculations must satisfy these relations.

In Fig. 2(b), we show the spin structure of the chains, and, in Fig. 2(c) reproduce the $m(H)$ data published elsewhere⁵. $m(H)$ has two steps, the first with a height of $2.8\mu_B/f.u.$ and the second, $4\mu_B/f.u..$ As T decreases, the spins align in the $\uparrow\downarrow\downarrow$ ordering⁴, and an anisotropic

next-nearest neighbor Ising (ANNNI) model¹² with alternating spins^{9,11,13} has successfully described many properties of CCMO⁸; here we apply it to $m(H)$ to resolve the spin-states. The Hamiltonian is

$$\mathcal{H} = \sum_i J_1 s_i S_i + J_2 S_i S_{i+1} + J'_2 s_i s_{i+1} - \mu_B H_z (g_s s_i + g_S S_i), \quad (1)$$

where s_i and S_i refer to Co and Mn spins in cell i respectively. The exchange couplings are given in Fig. 2(b), where J_2 and J'_2 are not identical; the sign of J_1 cannot be reliably determined from high T χ^{15} , and we find that both signs can reproduce $m(H)$ (Fig. 2(c) inset).

When analyzing $m(H)$ for $H||c$, it is useful to discuss moments, $\mu_z(Co, Mn)$, not spins and g-factors, where $\mu_z(Mn) = g_S S = 3$, and $\mu_z(Co) = g_s s$ is unknown. For $\mu_z(Co) < \mu_z(Mn)$, the ground states of (1) go from $\uparrow\downarrow\downarrow$ to $\uparrow\uparrow\downarrow$ to $\uparrow\uparrow\uparrow$ as H_z increases, yielding the $m(H)$ steps shown in Fig. 2(c); the ratio of plateau heights is

$$\frac{M_{plat}}{M_{sat}} = \frac{\mu_z(Mn)}{\mu_z(Mn) + \mu_z(Co)} = \frac{1}{1 + \frac{\mu_z(Co)}{\mu_z(Mn)}} = \frac{3}{4}, \quad (2)$$

where 3/4 is the experimental value from Fig 2c. The linear behavior and hysteresis⁵ below the first step are due to polarization domain walls, which are free spins¹⁶.

The presence of two steps in $m(H)$ demands two different moments. These plateaus can be easily explained within the LS scenario; here, as H increases it first flips the large (Mn) spin (at H_1) and later (at $H_2 > H_1$) the small (Co) one. The first step then has a value of $\mu_z(Mn) = 3\mu_B$; this is consistent with the measured value of $2.8\mu_B$; and neutron scattering has confirmed that the first plateau is the expected $\uparrow\uparrow\downarrow$ state⁵. The height of the second step gives $\mu_z(Co) = g_{Co} S_{Co} = 1.2\mu_B$, where $g_{Co} \geq 2$ due to the nonzero orbital moment; this is larger than that observed in neutron scattering⁴ but three times smaller than that associated with $S = \frac{3}{2}$. The HS scenario would instead give a second plateau height between $5.8 - 7.8\mu_B$, depending on the orbital moment, and the simple HS picture is inconsistent with $m(H)$. For completeness, we note that the final step can be explained with a HS Co by a tripling of the magnetic unit cell at high fields; this unlikely scenario requires a failure of the ANNNI model, but could be checked by neutron diffraction. Dimensional fluctuations have also been suggested to reduce the HS Co moment to its observed value⁶, but the equally large Mn moment is only suppressed by 5%. The combination of the neutron scattering and $m(H)$ data strongly implies a small Co moment.

We examine the theoretical situation of the Co ion more carefully; by using general considerations we can rule out the HS scenario and show that the LS scenario can account for both the small moment and large anisotropy. We treat only the lowest CF levels, $|L_z = \pm m, S_z\rangle$, assuming that these are well separated, and introduce both SO and Jahn-Teller(JT) as perturbations,

$$\mathcal{H} = -|\lambda| \vec{L} \cdot \vec{S} - \mu_B (\vec{L} + 2\vec{S}) \cdot \vec{H} - \delta JT(E_a - E_b), \quad (3)$$

where the negative SO term comes from the alignment of spin and orbital moments in hole ions. The JT term, $\delta JT(E_a - E_b)$ splits $|L_z = \pm m\rangle$ into $|a, b\rangle = \frac{1}{\sqrt{2}}(|m\rangle \pm | - m\rangle)$, quenching the angular momentum.

First we try to obtain a small effective moment at low T within the HS scenario; here the Hund's energy, J_H is larger than the CF splitting, Δ (see Fig. 2), and the “true” spin is $\frac{3}{2}$. The lowest ($L_z = \pm 1$) level is half-filled; however the $L_z = \pm 2$ level is partially occupied, leading to an orbital moment of $2\mu_B$. The ground-state is eightfold degenerate, and is split into four Kramers doublets by either SO or JT interactions. With only SO splitting, $J_z = L_z + S_z$ remains a good quantum number, and the larger J_z levels lie lowest (Fig. 3A). The ground state doublet has $J_z = \pm \frac{7}{2}$ with a moment $\mu_z = L_z + 2S_z = 5\mu_B$, while $\mu_x = 0$. Thermal mixing lowers the anisotropy, causing χ_c/χ_a to increase with decreasing T; however, μ_z decreases only slightly with T and is four times larger than the observed moment at $T \sim |\lambda| \approx \lambda_0/2S = 230K$ in HS Co¹⁷.

Clearly SO splitting cannot explain the small moment, but what about JT distortions, which will quench the orbital contribution? Though JT is a small effect, if present, in CCMO⁷, we consider the extreme case, $\delta JT \gg |\lambda|$ as an example. These four-fold degenerate $S = \frac{3}{2}$ levels will be further split by second-order effects (see Fig. 3B). The general form of this Hamiltonian is constrained by the trigonal ($S_z \rightarrow S_z, S_{\pm} \rightarrow e^{\pm i2\pi/3}S_{\pm}$) and time-reversal symmetries ($\vec{S} \rightarrow -\vec{S}$) that only allow operators of the form S_z^2 or S_+S_- . If we consider the virtual fluctuations into the other JT quartet, the energy shift will be $\Delta E = -|\langle a|H_{SO}|b\rangle|^2/\delta JT = -4\lambda^2 S_z^2/\delta JT$, lowering the $S_z = \pm \frac{3}{2}$ level to restore the anisotropy while preserving the spin-only moment, $\mu_z = 3\mu_B$ and $\mu_x = 0$. Still, this moment is more than two times too large. Moreover, this is a “best-case moment”; both thermal mixing and stronger SO coupling will only increase it, and these should be quite important. Even if we could change the sign of ΔE to lower the $S_z = \pm \frac{1}{2}$ doublet, perhaps by fluctuations into nearby CF levels, its $S = \frac{3}{2}$ origins mean that, while the c-axis moment is small, $\mu_z = 1\mu_B$, the basal plane moment, $\mu_x = 2\mu_B$ is large, the inverse of the observed anisotropy.

None of the possible HS states can simultaneously explain the low moment and Ising anisotropy at low Ts; however they describe the high T data well. Therefore we turn to the LS scenario at low T, and propose a spin-state crossover between 16K and 300K. To obtain such a crossover, the difference in energy scales $J_H - \Delta$ must be small and negative; the LS ground state is energetically selected, but the entropy, $S \sim \log(2S+1)$ favors the HS state at higher T. While SO splits both the HS and LS states into doublets, there are more HS states, closer together (as $\lambda = \lambda_0/2S$). We note that such spin-state crossovers have been observed before; the best-known example is LaCoO₃¹⁸, where the 3d⁶ Co³⁺ transitions from a $S = 0$ ground state to $S = 2$ at 500K¹⁸; this crossover has been characterized by many probes¹⁹⁻²¹ and serves

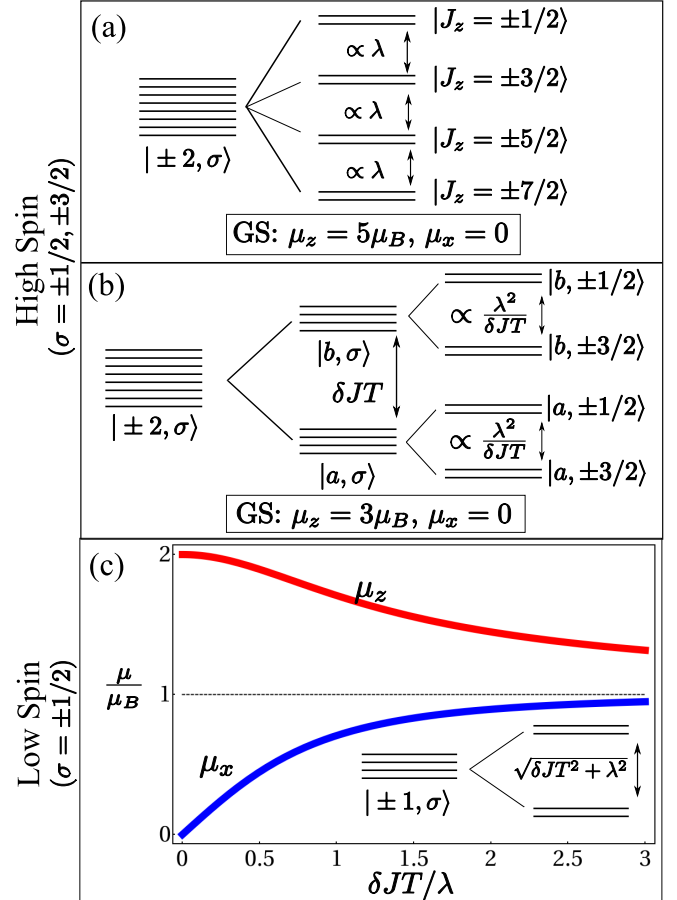


FIG. 3: Spin orbit(SO) and Jahn Teller(JT) distortions reduce both the $S = \frac{3}{2}, L_z = \pm 2$ (HS) octet and $S = \frac{1}{2}, L_z = \pm 1$ (LS) quartet to Kramer’s doublets, but with a range of moments and anisotropies. (A.) HS SO split states: as Co²⁺ is more than half filled, SO aligns the spin and orbital moments. (B.) HS JT split states: JT splits $| \pm m \rangle$ into $|a, b\rangle \equiv \frac{1}{\sqrt{2}}(|m\rangle \pm |-m\rangle)$, quenching $\langle \vec{L} \rangle$; but the anisotropy is restored by second-order SO effects, which favor the $S_z = \pm \frac{3}{2}$ level for small δJT . (C.) For the LS case, we allow $\delta JT/\lambda$ to vary, splitting the quartet into doublets, with the ground state ranging from perfectly anisotropic, $\mu_z = 2\mu_B, \mu_x = 0$ for pure SO to an isotropic $S = \frac{1}{2}$ for pure JT.

as a benchmark in our present discussion. Co²⁺ spin state transitions have been confirmed in several organic complexes²² at lower Ts, but never in a crystal. In these materials the Co ions are in octahedral symmetries, but no spin-state transitions have yet been observed in trigonal coordination, where the CF splitting, Δ is generally smaller (see Fig. 2); however density functional theory on the related Ca₃Co₂O₆ indicates that there Δ is nearly as large as in octahedral geometry²³. Although first principles calculations on CCMO have found HS Co^{6,7}, we believe their J_H may be too large. Having eliminated the HS scenario, we next pursue the exotic LS scenario.

The LS state has spin $\frac{1}{2}$, but there is also an un-

quenched angular momentum, $L_z = \pm 1$ from the partially occupied level. Both SO and JT split this quartet into two Kramers doublets, and we have treated these simultaneously, plotting the ground state μ_z and μ_x for a range of $\delta JT/\lambda$ (Fig. 3 C). The pure SO case leads to a $J_z = \pm \frac{3}{2}$ doublet, with maximum anisotropy at $T = 0$, while the pure JT case leads to an isotropic spin $\frac{1}{2}$ at zero T, with increasing anisotropy with T . It is impossible to get both a low moment and a large anisotropy from CFs alone in a hole ion; while SO gives rise to the anisotropy, it also always aligns the orbital and spin moments.

In spin chains, the magnetic fluctuations extend over a large temperature range and cannot be neglected. As magnetism develops along the chains, the spins align and the anisotropy increases; the $\uparrow\uparrow\downarrow\downarrow$ order also leads to exchange striction, causing a nonzero polarization. It likely also distorts the trigonal environment of the Co, thus acting as a small JT distortion to reduce the moment. The concurrent JT reduction of the anisotropy will be small compared to the positive magnetic contribution, and thus this combination of low-dimensional magnetic fluctuations and exchange striction will lead to a smaller moment while maintaining the large spin anisotropy.

We therefore propose the following scenario: at the lowest temperatures, Co is in a spin $\frac{1}{2}$ state, where the orbital moment is partially quenched by exchange striction associated with the developing magnetism. Entropy favors the spin $\frac{3}{2}$ state with a large orbital moment, leading to a spin-state crossover between $T^* = 16K$ and room T. This scenario provides a coherent explanation of *all* the experimental evidence, at both low and high T.

The spin state transitions in LaCoO₃ are clearly visible as a decrease in the effective moment¹⁹, while CCMO features only a weak upturn in χ_c^{-1} , seemingly indicating an increase of the moment, and a downturn in χ_{ab}^{-1} . However, in LaCoO₃, the magnetism comes solely from the HS states, while there are several competing effects in CCMO. The development of magnetism along the chains increases the effective Co and Mn c-axis moments, causing an upturn in χ_c^{-1} , while the increasing anisotropy of the Mn spin reduces its ab-plane moment, explaining the

downturn in χ_{ab}^{-1} . Thermal population of the SO split levels(see Fig. 3 A,C) also increases $\mu_z(Co)$ as the temperature decreases, with effects down to one third of the SO coupling, near the observed upturn at 150K¹⁵. Either of these could mask a decreasing moment; moreover, if the Weiss temperature does not reduce with the moment, a spin state crossover will manifest as an upturn in χ_c^{-1} above the crossover temperature followed by a downturn. For these reasons, the upturn in χ_c^{-1} does not rule out a LS-HS crossover, but it does suggest that the crossover, if it occurs, is at or below 100K.

The most direct experimental test of the spin-state crossover would be to probe the LS ground state with XAS at low T; this method was used to confirm the spin-state crossover in LaCoO₃²⁰. There are also several other consequences of the spin-state transition. The excitation between the LS and HS states is observable in inelastic neutron scattering. Another magnetization plateau at $5.8 - 7.8\mu_B/f.u.$ will occur at higher fields which favor the HS state. Finally, as the Co ion volume increases with increasing degeneracy²⁴, a pressure-dependent spin state crossover should occur in CCMO at fixed T.

In conclusion, we have analyzed the field-dependent magnetization and the magnetic anisotropy in CCMO to prove that at low temperatures the Co²⁺ ions are unambiguously in a spin $\frac{1}{2}$ state with a moment consistent with earlier neutron studies⁴. Similarly, high temperature studies⁶ indicate that this same ion is unambiguously spin $\frac{3}{2}$. We have shown that this small moment, in combination with the observed anisotropy, cannot be reconciled with a high spin scenario by invoking spin-orbit coupling or Jahn-Teller distortions. We thus propose a low spin-high spin crossover as a function of temperature and suggest a number of experimental probes to test this idea.

We acknowledge helpful discussions with P. Coleman, M. Croft, M. Dzero, M. Haverkort and A. Nevidomskyy. The susceptibility was measured by Y.J.Chi. This work was supported by DOE DE-FG02-99ER45790(RF),DOE DE-FG02-07ER46832(HY,SC,VK) and NSF-NIRT-ECS-0608842(PC).

* Electronic address: flint@physics.rutgers.edu

¹ S-W. Cheong and M. Mostovoy, Nat. Mater. **6**, 13(2007).

² V.G. Zubkov et al, J. Solid State Chem. **160**, 293(2001).

³ S. Rayaprol et al., Sol. State Comm. **128**, 79 (2003).

⁴ Y.J. Choi et al, Phys. Rev. Lett. **100**, 047601(2008).

⁵ Y.J. Jo et al., Phys. Rev. B **79**, 012407(2009);

⁶ H. Wu et al, Phys. Rev. Lett. **102**, 026404 (2009).

⁷ Y. Zhang et al.Phys. Rev. B **79**, 054432(2009).

⁸ X.Yao and V.C. Lo, J. Appl. Phys. **106**, 013903(2009).

⁹ V. Kiryukhin et al., Phys. Rev. Lett. **102**, 187202(2009).

¹⁰ T. Lancaster et al., Phys. Rev. B **80** 020409 (1990).

¹¹ M.G. Pini and A. Rettori, Phys. Rev. B **48**, 3240(1993).

¹² P. Bak, Rep. Prog. Phys. **45**, 587(1982).

¹³ J. Kim et al, J. Phys. Soc. Jap. **65**, 2624(1996).

¹⁴ D. Dai and M.-H. Whangbo, Inorg. Chem. **44**,12(2005).

¹⁵ M. W. Haverkort et al,arXiv.org:0806.3736(2008).

¹⁶ A polarization domain wall: $\uparrow\downarrow\downarrow\downarrow\uparrow\uparrow\uparrow$ contains two free(E=0) spins(underlined).

¹⁷ P. Fazekas, *Lecture Notes on Electron Correlation and Magnetism*(World Scientific,Singapore, 1999)

¹⁸ W.C. Koehler and E.O. Wollan, J. Phys. Chem. Sol. **2**, 100(1957);
J.B. Goodenough et al., J. Phys. Chem. Sol. 5, 17 (1958).

¹⁹ C.S. Naiman et al., J. Appl. Phys. **36** 1044(1965).

²⁰ M. W. Haverkort et al, Phys. Rev. Lett. **87**, 176405(2006).

²¹ D.P. Kozlenko et al., Phys. Rev. B 75, 064422 (2007).

²² H.A. Goodwin, *Topics in Current Chemistry* **234**, 23(2004).

²³ H. Wu et al., Phys. Rev. Lett. **95**, 186401(2005).

²⁴ R. Bari and J. Sivardiere, Phys. Rev. B **5**,4466(1972).